Published online 3 October 2008

Nucleic Acids Research, 2008, Vol. 36, No. 21 ***e140***
doi:10.1093/nar/gkn634

The application of real-time PCR to the analysis of T cell repertoires

Peter Wettstein[1,2,*], Michael Strausbauch[1,2], Terry Therneau[3] and Nancy Borson[1,2]

[1]Department of Immunology, [2]Department of Surgery and [3]Department of Health Sciences Research, Mayo Clinic College of Medicine, Rochester, MN 55905, USA

Received June 5, 2008; Revised September 4, 2008; Accepted September 6, 2008

ABSTRACT

The diversity of T-cell populations is determined by the spectrum of antigen-specific T-cell receptors (TCRs) that are heterodimers of α and β subunits encoded by rearranged combinations of variable (AV and BV), joining (AJ and BJ), and constant region genes (AC and BC). We have developed a novel approach for analysis of β transcript diversity in mice with a real-time PCR-based method that uses a matrix of BV- and BJ-specific primers to amplify 240 distinct BV–BJ combinations. Defined endpoints (Ct values) and dissociation curves are generated for each BV–BJ combination and the Ct values are consolidated in a matrix that characterizes the β transcript diversity of each RNA sample. Relative diversities of BV–BJ combinations in individual RNA samples are further described by estimates of scaled entropy. A skin allograft system was used to demonstrate that dissection of repertoires into 240 BV–BJ combinations increases efficiency of identifying and sequencing β transcripts that are overrepresented at inflammatory sites. These BV–BJ matrices should generate greater investigation in laboratory and clinical settings due to increased throughput, resolution and identification of overrepresented TCR transcripts.

INTRODUCTION

The diversity of T-cell repertoires is dependent on the range of combinations of unique α and β subunits that determine the antigenic specificity of T-cell receptors (TCRs). This specificity is determined by the utilized variable (V) and joining (J) regions in α and β subunits as well as the diversity (D) regions in β subunits (1). Recombinations between V and J gene segments result in the formation of complementarity-determining region 3s (CDR3s) that include the carboxy and amino termini of the V and J segments, respectively, as well as variable numbers of random nucleotides inserted between the V and J segments. CDR3s impact antigenic specificity through their lengths and amino acid sequences (2–5) that contact the amino and carboxy termini of peptides that are bound to the products of major histocompatibility complex (MHC) class I and class II genes (6). Analysis of the diversities of TCR repertoires has been aimed at (i) quantitating the diversity of α and β transcripts within T-cell populations and (ii) identifying and sequencing overrepresented TCR transcripts. A number of methods have been developed to evaluate diversity through quantitation of the speed and efficiency of rehybridization of denatured PCR products from populations of β transcripts (7,8) and hybridization of cRNA from β transcripts to arrays of expressed sequence tags from human genes (9). The identification of overrepresented TCR transcripts involves (i) the cloning and sequencing of β transcript sequences from selected populations of cDNA or PCR products and/or (ii) the cloning of T cells followed by amplification and sequencing of TCR transcripts.

The only experimental platform that both evaluates TCR diversity and identifies prominent β transcripts is spectratyping, or immunoscope, that is based on the observations that transcripts carrying a single BV or AV gene segment normally include CDR3s that exhibit Gaussian distributions of length. This method involves reverse transcriptase-polymerse chain reaction (RT–PCR) amplification of α and β transcripts using V gene-specific forward primers and a constant region reverse primer followed by electrophoretic separation of amplicons for the display of distributions of CDR3 lengths (10–12). Spectratyping has been useful for two purposes: (i) evaluation of diversity since TCR transcripts from normal T-cell populations display Gaussian distributions of CDR3 lengths whereas amplicons from selected populations can exhibit reductions in variability of CDR3 lengths due to restrictions in diversity and/or antigen-driven expansion of specific T cells (12) and (ii) identification of amplicons with single CDR3 lengths for direct sequencing that can be successful if a single amplicon is present for a single V gene primer (12–14). BJ-specific primers have been selected for increased resolution

*To whom correspondence should be addressed. Tel: +1 507 284 9654; Fax: +1 507 284 3757; Email: wettstein.peter@mayo.edu

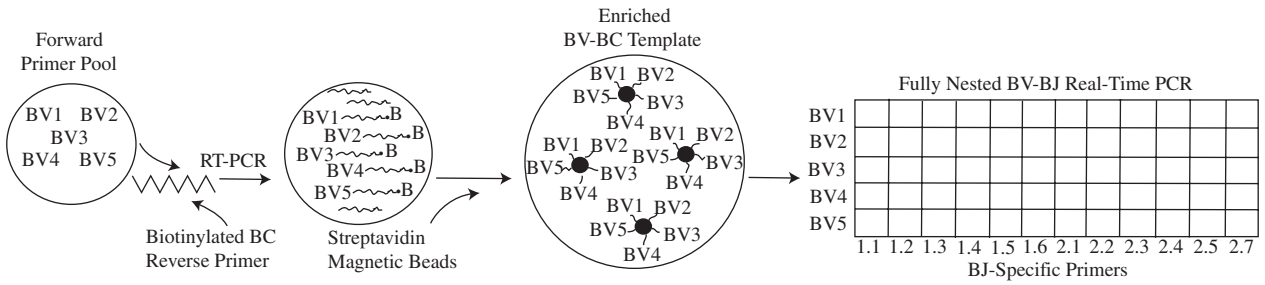

Figure 1. Schematic diagram of pooled RT–PCRs and BV–BJ-specific real-time PCRs.

through re-amplification of BV–BC amplicons (15,16), but these BV–BJ re-amplifications have not been utilized for the routine analysis of TCR diversity. The identification and sequencing of overrepresented transcripts at inflammatory sites, tumors, and transplanted organs, can provide important data for understanding the diversity of T-cell populations at those sites as well as characteristics of CDR3 regions expressed by the overrepresented T cells.

Despite the capacity of spectratyping to both evaluate diversity and antigen-driven selection, technical complexities appear to have limited its wide-spread application, as evidenced by the drive to develop the alternative, hybridization-based approaches described above (7–9). Methods that utilize quantitative (real-time) RT-PCR have more recently been developed to quantitate the relative percentages of T cells that express individual BV genes (17,18), but these methods lack the resolution required to effectively evaluate repertoire diversity and efficiently identify overrepresented transcripts due to their BV gene-specific amplifications. The capacity of real-time PCR methodology to simultaneously monitor amplification in multiple reactions with high sensitivity offers an opportunity to develop TCR repertoire analysis with improved levels of resolution, speed and cost. In this communication, we describe a real-time PCR method that is designed to individually and simultaneously amplify all 240 BV–BJ combinations expressed by murine T cells. The increased complexity of this matrix of 240 combinations increases the resolution of the analysis of repertoire diversity as well as the efficiency of identification and sequencing of overrepresented transcripts.

MATERIALS AND METHODS

Mice

C57Bl/10SnJ (B10), C57BL/6J (B6), B10.129-*H4*^{b} (21M), and NOD.CB17-*Prkdc*^{scid}/J (NOD-scid) mice were purchased from the Jackson Laboratory (Bar Harbor, ME). BALB/c-nude mice were purchased from Taconic Farms, (Germantown, NY, USA). All mice were housed in the barrier facility in the Mayo Clinic Department of Comparative Medicine, and all mice were raised and maintained with protocols approved by the Institutional Animal Care and Use Committee of the Mayo Clinic.

Cell harvests and skin grafting

Lymphocyte populations were suspended by pressing spleens through nylon bolting cloth (100 μm pore size); lymphocytes were resuspended in lysis buffer (RNeasy Protect MiniKit, Qiagen, Valencia, CA, USA) for storage at −80°C. T cells were enriched from spleen cell suspensions from nude mice by panning over dishes coated with affinity-purified goat anti-mouse immunoglobulin as previously described (19). Transplantation of orthotopic tail skin grafts (~2 × 5 mm^2 in size) was performed according to the previously described technique (20). All skin grafting was performed with donors and recipients that were anesthetized with sodium pentobarbital. Each recipient of primary allografts received a single autograft and two allografts. Second through fifth sets of two skin allografts were transplanted ~14 days after rejection of the preceding set of allografts. Fifth set grafts were harvested during the process of rejection, and harvested grafts were immediately transferred to lysis buffer for storage at −80°C.

Experimental method for β transcript amplification

Murine TCR β transcript repertoires include transcripts that result from rearrangements between 21 BV and 12 BJ gene segments. The described method ultimately involves the simultaneous amplification of 240 BV–BJ combinations by real-time PCR using 20 BV- and 12 BJ-specific primers (Figure 1). Briefly, β transcripts are first reverse-transcribed from total RNA with a biotinylated BC region reverse primer and amplified with pools of BV-specific forward primers. The resulting amplicons are mixed with streptavidin-coated magnetic beads to enrich products that include the biotinylated BC region primer. The bead-enriched products are delivered to microtiter wells for amplification in real-time PCR using 240 nested BV–BJ primer pairs.

Extraction of total RNA

Total RNA was extracted from suspended splenocytes and tail skin grafts from individual mice using an RNeasy Protect MiniKit (Qiagen) according to the manufacturer's instructions. Approximately 0.6 μg and 1.5–5.0 μg total RNA were extracted per million splenocytes and two skin grafts, respectively. Residual genomic DNA was removed from extracted RNA samples using an RNase-Free DNase Set (Qiagen). Total RNA was diluted to 5 ng/μl in water immediately prior to use in RT–PCRs.

Table 1. Sequences of oligonucleotide primers used for amplifications in pooled RT–PCRs and real-time PCRs

RT–PCR primers			
Constant region reverse primer: Bio-GCAATCTCTGCTTTTGATGGCT (Biotinylated at 5′-end)			
	Pool #1:		**Pool #2:**
BV1	TATGTCTTGTGGAAACAGCACTC	BV4	GAAAAAATCCTGATATGCGAACAGTA
BV2	ATGGCTTCTGTGGCTACAGACC	BV6	CAAAAACTGACCTTGAAATGTCAA
BV5.1	AACACTGCCTTCCCTGACCC	BV7	AGAATGTTTTGCTGGAATGTGGA
BV5.2	GTCTAACACTGTCCTCGCTGATTC	BV11	TGCTTCTTGAGAGCAGAACCAA
BV8.3	GAAAGGTGACATTGAGCTGTCAC	BV12	CAATAATCCTGAAGTGTGAGCCAG
	Pool #3:		**Pool #4:**
BV3	AAGGACAAAAAGCAAAGATGAGG	BV8.1	GAAAGGTGACATTGAGCTGTCAC
BV14	CCTGGGCATGTTCTTGGG	BV8.2	GGAAAGGTGACATTGAGCTGTAAT
BV15	TATTACTTCTGGGGCCTG	BV9	CTTCTGTCTTCTTGCAGCCACTT
BV16	GTTGGATAATTTTTAGTTTCTTGGAAG	BV10	TGCCTCTTGGGAATAGGCC
BV20	GGCCAGGAAGCAGAGATGAAA	BV13	AGTGTTCTGTCTCCTTGACACAGTAC
		BV18	CCTGCTACTTCTTTGGAGCCA
Real-time PCR primers			
	Nested BV primers		**BJ primers**
BV1	GCCCAGTCGTTTTATACCTGAAT	BJ1.1	CTGGTTCCTTTACCAAAGAAGACT
BV2	GTGCTGATTACCTGGCCACAC	BJ1.2	CCCTGAGCCGAAGGTGTAGTC
BV3	GAAAAACGATTCTCTGCTGAGTGT	BJ1.3	TTCTCCAAAATAGAGCGTATTTCC
BV4	CTTATGGACAATCAGACTGCCTCA	BJ1.4	GGTTCCATGACCGAAAAATAATCT
BV5.1	ATGGAGAGAGATAAAGGAAACCTG	BJ1.5	CTCCAAAAAGCGGAGCCTG
BV5.2	GTGGAGAGAGACAAAGGATTCCTA	BJ1.6	CGCAAAGTAGAGGGGCGAA
BV6	GGCGATCTATCTGAAGGCTATGA	BJ2.1	CTGGTCCGAAGAACTGCTCA
BV7	AAGGAGACATCCCTAAAGGATACAG	BJ2.2	CCAAAGTAGAGCTGCCCGGT
BV8.1 + 2	CAAGGCCTCCAGACCAAGC	BJ2.3	CCTGAGCCAAAATACAGCGTT
BV8.3	ACAAGGCCACCAGAACAACG	BJ2.4	GCACCAAAGTACAAGGTGTTTTG
BV9	TTCTACTATGATAAGATTTTGAACAGGG	BJ2.5	GGCCCAAAGTACTGGGTGTC
BV10	GGCGCTTCTCACCTCAGTCTT	BJ2.7	GCCGGGACCGAAGTACTGT
BV11	AGATGATTCAGGGATGCCCA		
BV12	CAAGTCTCTTATGGAAGATGGTGG		
BV13	GATGAG GCTGTTATAGATAATTCACAGT		
BV14	CAGGTAGAGTCGGTGGTGCAA		
BV15	CAGGAAAAATTTCCCATCAGTCAT		
BV16	GGAGAAGTCTAAACTGTTTAAGGATCAG		
BV18	AAGGACAAGTTTCCAATCAGCC		

Primers

The RT–PCRs and real-time PCRs required the following primers: (i) a reverse BC region primer that was biotinylated at the 5′- end, (ii) a pair of nested forward primers specific for each of the 21 individual BV genes and (iii) a set of reverse primers specific for the 12 individual BJ genes (Table 1). Sequences of 21 forward, outer BV primers are homologous to sequences within the CDR1 regions of BV genes, and these primers are divided into four primer pools based on relative homologies. Twenty nested BV primers are based on sequences within the CDR2 regions. The relatively high homology between BV8.1 and BV8.2 genes was problematic for discriminating amplification. Although the BV8.1- and BV8.2-specific primers for RT–PCRs were distinguished by two nucleotide substitutions in the first four nucleotides at the 3′-ends, we were not confident of their capacities to distinguish BV8.1 and BV8.2 genes. Considering the technical complexities in setting up real-time PCRs with such a large matrix, we chose to place the BV8.1- and BV8.2-specific outer primers in the same pool for RT–PCRs and co-amplify them with a single inner primer in real-time PCRs. All primers were synthesized by the Invitrogen (Carlsbad, CA,USA) Supply Center located at the Mayo Clinic Primer Core Facility (Rochester, MN, USA). The biotinylated BC region reverse primer was diluted to 20 μM in water. Outer, forward BV primers for RT–PCRs were mixed in four pools: three pools of five primers and one pool of six primers. The concentration of each primer in a pool was adjusted to 6.6 μM in water. BV- and BJ-specific primers for real-time PCRs were diluted to 10 μM in water.

RT–PCRs

RNA templates were denatured at 75°C for 4 min and placed on ice prior to addition to RT–PCR reactions. Four pooled RT–PCRs were performed in 25 μl volumes using (i) a master mix from a one-step RT–PCR Kit (Qiagen; 20 μl), (ii) 15 ng of denatured total RNA (3 μl), (iii) 20 pmol of a 5′-biotinylated BC primer (1 μl) and (iv) 6.6 pmol of each of the pooled BV primers (1 μl of pooled primers). RT–PCRs were performed on a PTC-225 Peltier Thermal Cycler (MJ Research, Waltham, MA, USA) as follows. cDNA was synthesized at 50°C for 32 min followed by incubation at 95°C for 15 min to inactivate the reverse transcriptase. Subsequent PCR

parameters were 1 min at 94°C, 30 s at 60°C, and 1 min at 72°C for 25 cycles. A final extension cycle was performed for 6 min at 72°C. RT–PCR products were separated from residual primers and amplification reagents using a QIAquick PCR Purification Kit (Qiagen) and eluted with 50 µl of elution buffer.

Enrichment of biotinylated PCR products

Biotinylated RT–PCR products were enriched with magnetic My One™ Streptavidin C1 Dynabeads (Dynal Biotech ASA, Oslo, Norway) using the manufacturer's magnet and protocol. For each RT–PCR product, 50 µl of Dynabeads were washed 2-times in 50 µl of 2× washing and binding buffer [10 mM Tris–HCl (pH 7.5), 1 mM EDTA, and 2 M NaCl]. The washed beads were resuspended in 100 µl of 2× washing and binding buffer and added to 50 µl of sterile water and the RT–PCR product (50 µl). The bead + product suspensions were gently shaken at room temperature for 15 min. The product-bound beads were washed twice with 100 µl of 1× washing and binding buffer and then resuspended in 100 µl of 10 mM Tris–HCl, pH 8.5. Suspensions of amplicon-bound beads were diluted 1:10 immediately prior to use as templates in real-time PCR reactions.

Real-time PCR

A total of 240 individual real-time PCRs (20 BV and 12 BJ primers) were performed in 10 µl volumes in 384-well Clear Optical Reaction Plates with Optical Adhesive Covers (Applied Biosystems, Foster City, CA, USA). The components of reactions were (i) 5 µl of Power SYBR Green PCR Master Mix (2×) (Applied Biosystems), (ii) 1 µl of the respective amplicon-bound bead suspension, (iii) 10 pmol of a nested BV primer (1 µl) and (iv) 10 pmol of a BJ-specific primer (1 µl) and 2 µl of nuclease-free water (Qiagen). Cycling was performed on an ABI Prism 7900HT Sequence Detection System at the AGTC Microarray Shared Resource Core Facility (Mayo Clinic Rochester, MN, USA) using SYBR Green detection. Cycling parameters were as follows: (i) an initial incubation at 50°C for 2 min, (ii) a 10 min incubation at 95°C to activate the DNA polymerase and (iii) 40 cycles of 15 s at 95°C followed by 1 min at 60°C. Dissociation curves were generated by (i) incubating the amplicons at 95°C for 15 s, (ii) reducing the temperature to 60°C for 15 s and (iii) increasing the temperature to 95°C over a dissociation time of 20 min. Data were analysed with the 7900HT Sequence Detection System (SDS) Version 2.3 software (Applied Biosystems) to estimate cycle threshold (Ct) values and dissociation curves to estimate the optimal melting temperatures for all reactions. Ct values are fractional cycle numbers at which fluorescence equals the threshold level (designated by a horizontal line in Ct plots), that is automatically set to be within the exponential region of the amplification curve where there is a linear relationship between the log of change in fluorescence and cycle number. Dissociation curves are formed by plotting rising temperatures versus the change in fluorescence/change in temperature.

Sequence analysis

Real-time PCR products were cleaned using a QIAquick PCR Purification Kit prior to sequencing with 2 pmol of the respective, nested BV primers. Sequencing was performed by the Mayo Clinic Molecular Biology Core Facility using a Big Dye Terminator v1.1 Cycle Sequencing Kit (Applied Biosystems) prior to sequence analysis with a 96-capillary ABI PRISM™ 3730 XL DNA Analyzer (Perkin Elmer Applied Biosystems, Foster City, CA, USA) by the Mayo Clinic Molecular Biology Core Facility.

Statistical analysis

The relative abundance of BV–BJ combinations was defined by the observed Ct values. Dissociation curves were used to confirm the presence of amplicons from β transcripts by excluding (i) primer-dimers that had relatively low melting temperatures and (ii) amplicons with dissociation peak heights that did not exceed a threshold of 0.07 (change in fluoresence/change in temperature). This threshold was selected experimentally due to the inability to sequence amplicons that were below this value. Amplicons with either or both of these characteristics were assigned Ct values of >40 cycles. The diversities of the 240 BV–BJ combinations within individual RNA templates were estimated by Shannon entropy (21) that has been used for estimating variability at individual amino acid positions in immunoglobulin variable region (V) gene products (22). An estimate of scaled entropy (H) was calculated for each BV–BJ matrix by the equation $H = \Sigma(P \log_2 P)/\log_2(1/240)$ where P was the probability of abundance calculated for each BV–BJ combination by the equation $P = 2^{-y}/\Sigma 2^{-y}$ where y was the Ct value for the BV–BJ primer pair and $P = 0$ when Ct > 40 cycles.Scaled entropy ranges from 0 to 1 with 1 representing maximal diversity.

RESULTS

Experimental method

The diversity of expressed combinations of individual BV and BJ genes is a major contributor to the diversity of TCR repertoires. Two hundred and fifty-two BV–BJ combinations can be expressed in mice based on 21 BV and 12 BJ genes. A real-time PCR matrix was developed to evaluate expression of transcripts carrying 240 different BV–BJ combinations using 20 BV primers and 12 BJ primers. The BV8.1 and BV8.2 genes were grouped together due to their relatively high level of homology. The flow of the experimental method is presented in Figure 1. Templates for real-time PCRs were amplified in four pooled RT–PCRs using (i) total RNA as template, (ii) a reverse constant region primer that was biotinylated at the 5′ end and (iii) four pools of five to six BV-specific primers. RT–PCRs were performed with pooled BV primers to conserve total RNA, and BV-specific primers were placed in pools on the basis of relative homology to minimize cross-priming. Excess primers were washed from amplified products by direct column purification prior

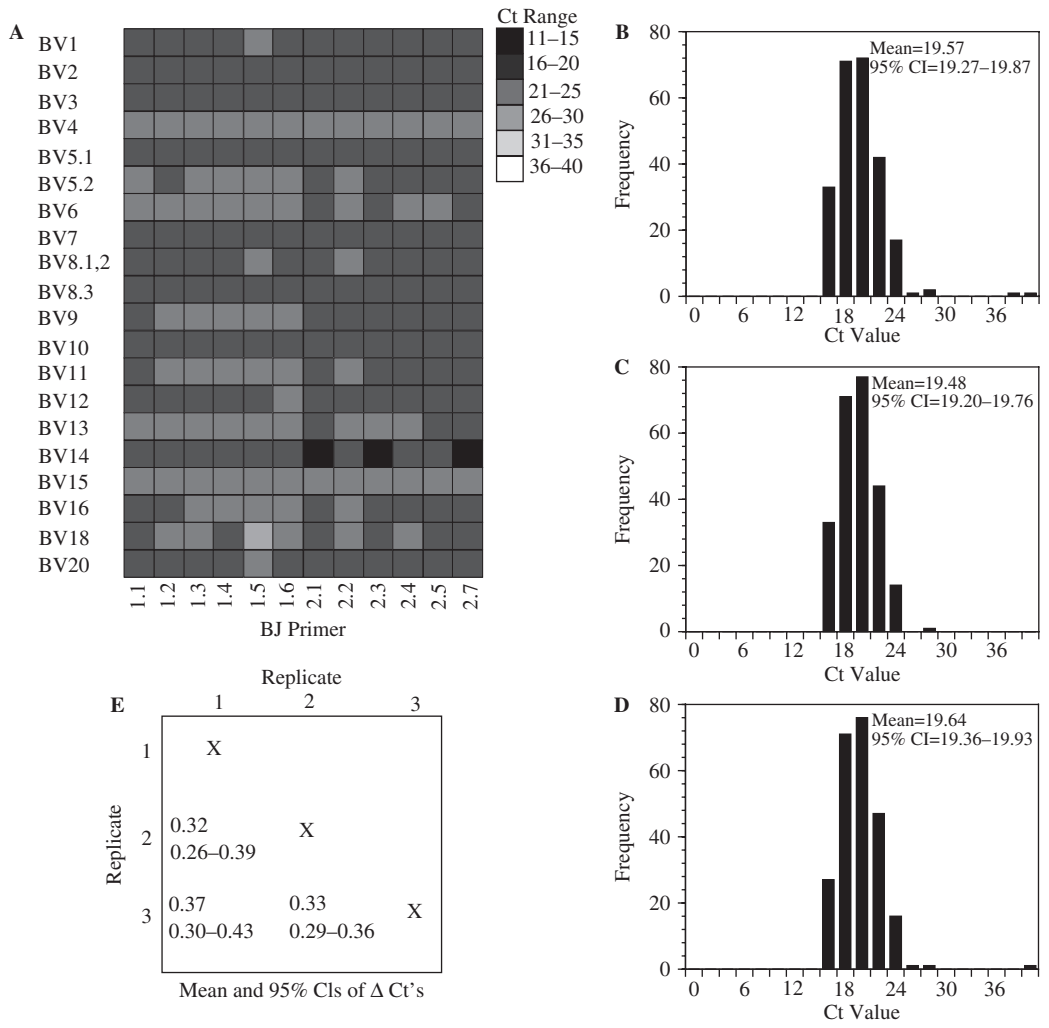

Figure 2. Distribution of Ct values from 240 BV–BJ combinations and reproducibility of BV–BJ-specific amplification. (**A**) Representation of the distribution of Ct values using total RNA template extracted from normal B6 splenocytes. Histograms of the distributions of Ct values from (A) (**B**) and two replicate amplifications (**C** and **D**) of the same RNA template with notations of the mean Ct values and 95% confidence intervals (CIs) of the means. (**E**) Mean ΔC_t values and 95% CIs for pairwise comparisons of Ct values from 240 BV–BJ combinations in the three replicate amplifications.

to their addition to streptavidin-coated magnetic beads to enrich products carrying the biotinylated BC primer. Bead-based enrichment of RT–PCR products was included in the method rather than simple dilution of the products since it was shown to increase specificity in the downstream real-time PCRs (data not shown), presumably due to the elimination of non-specific products derived from non-specific pairing of the pooled BV primers.The selections of numbers of cycles in RT–PCRs and the extent of dilution of bead-enriched products were interrelated and determined by (i) the numbers of BV–BJ primer pairs for real-time PCRs, (ii) the range in representation of transcripts carrying different BV–BJ combinations and (iii) the minimization of the numbers of amplicon-bound beads added to real-time PCRs. Amplicon-bound beads were diluted and aliquoted into the wells of 384-well plates along with 240 combinations of nested BV- and BJ-specific primers.

Amplification was monitored by the uptake of SYBR Green with automated estimation of Ct values throughout each reaction. Dissociation curves were generated after the final amplification cycle by increasing.the temperature from 60–95°C. The selection of SYBR Green to monitor amplification was based on the difficulty and expense in designing and synthesizing fluorochrome-labeled probes for individual BV genes. SYBR Green also allows analyses of dissociation peak shapes to visually distinguish products of single and multiple transcripts. Lack of specific amplification was concluded if: (i) SYBR Green uptake had not reached the threshold for estimation of a Ct value: (ii) there had been a low melting temperature that was not characteristic of β transcript products: or (iii) heights of dissociation peaks did not exceed a threshold of 0.07 (change in fluorescence/change in temperature). In such cases, Ct values of >40 cycles were assigned.

TCR repertoires in normal mice

BV–BJ matrices were first used for the analysis of β transcript repertoires in lymphocyte populations from normal mice. The data presented in Figure 2A were derived from

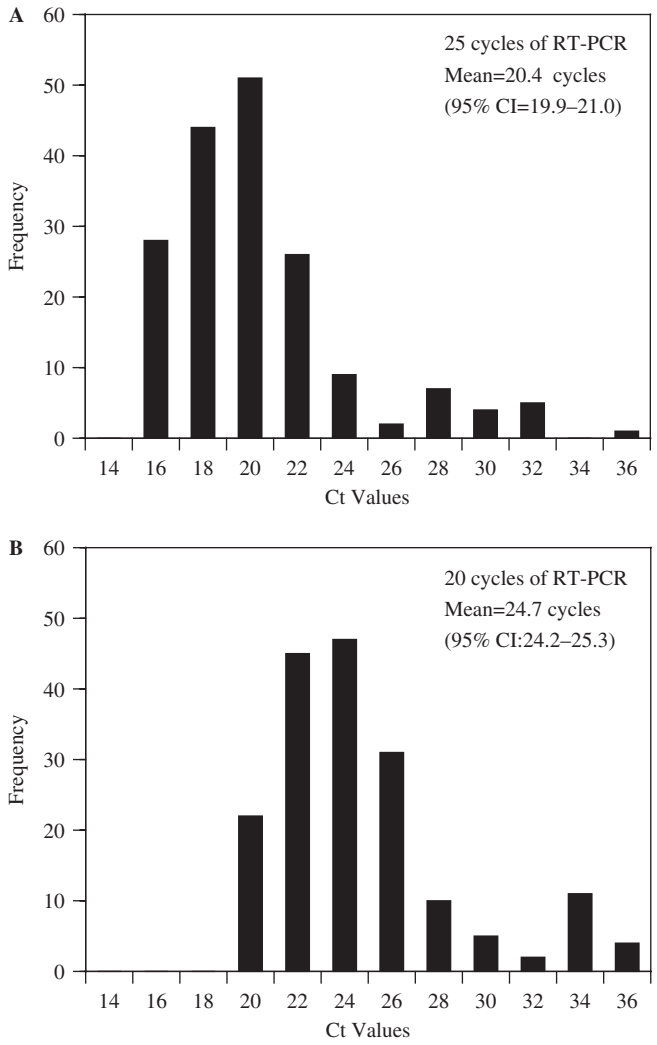

Figure 3. Effects of decreasing numbers of RT–PCR cycles on mean Ct values in BV–BJ real-time PCRs. (**A**) Distribution of Ct values following 25 cycles of RT–PCR and (**B**) distribution of Ct values following 20 cycles of RT–PCR.

the amplification of total RNA extracted from splenocytes harvested from a single B6 mouse; 15 ng RNA were used for each pooled RT–PCR. Ct values were estimated for each BV–BJ combination, taking into consideration the dissociation curves to confirm the amplification of β transcripts and exclude primer-dimers based on the curves of melting temperatures. The threshold for Ct value estimation was reached with all BV–BJ combinations and all melting curves were consistent with amplification of β transcripts. The vast majority of Ct values (95%) were between 16 and 24 cycles (Figure 2A and B). These results demonstrate that all 240 BV–BJ combinations can be amplified with the utilized primer sets.

Amplification in a total of 25 RT–PCR cycles and 40 real-time PCR cycles requires careful attention to potential sources of experimental error. Two additional replicate assays were performed with the same source of RNA template to evaluate reproducibility (Figure 2C and D). The mean Ct values for the replicate matrices (19.57 and 19.64) were virtually identical to that of the original matrix (19.48 cycles) with comparable distributions. The replicate distributions of Ct values were also compared by calculating (i) the delta Ct (ΔC_t) values between individual, replicate BV–BJ combinations and (ii) the mean ΔC_ts for all three comparisons of replicate matrices. The mean ΔC_ts ranged from 0.32 to 0.37 (Figure 2E), and these ranges are well within the sensitivity range of ±0.5 cycles reported with the use of gene expression master mixes for real-time PCR (personal communication, Applied Biosystems). The effects of different lymphocyte sources of total RNA on the reproducibility of results from BV–BJ matrices can be assessed by comparing the mean Ct values, described in Figures 2–5, that were obtained with RNA extracted from splenocytes harvested from multiple C57 background mice.

The amplification of β transcripts with outer BV primers in RT–PCRs increases the specificity of amplifications in fully nested BV–BJ-specific real-time PCRs. However, RT–PCR amplifications through 25 cycles could potentially lead to saturated product levels which could distort the distributions of β transcript products and, therefore, alter the results of the BV–BJ matrix. Therefore, we investigated the effects of reducing the number of RT–PCR cycles on mean Ct values from BV–BJ primer pairs in real-time PCRs. RNA template (15 ng) from normal B6 splenocytes was amplified for 20 and 25 cycles in RT–PCRs. Amplified products were bead-enriched and amplified with 180 BV–BJ primer pairs in real-time PCRs. The reduction of the RT–PCRs to 20 cycles resulted in an increase in mean Ct value of 4.3 cycles (Figure 3). These results suggested that the accumulation of products in the RT–PCRs was not saturated over the 20–25 cycle range.

Effects of dilutions of templates for RT–PCRs and real-time PCRs

BV–BJ primer pairs with comparable efficiencies are important for maximal detection of transcripts with variable levels of representation. Comparable primer pair efficiencies should yield comparable increases in Ct values following dilution of templates for real-time PCRs. Pooled RT–PCRs were performed and the bead-enriched products from each pooled RT–PCR were used in real-time PCRs undiluted (as per standard protocol) and diluted 1/4 and 1/16 (Figure 4). A 1/4 dilution resulted in a mean increase of 1.29 cycles and a 1/16 dilution resulted in an additional mean increase of 1.68 cycles (Figure 4A–C). More importantly, >90% of the BV–BJ combinations exhibited ΔC_t values in the 1.0–1.75 cycle interval in the undiluted versus 1/4 comparison, and, likewise, >90% of the combinations showed ΔC_t values in the 1.25–2.00 interval for the 1/4 versus 1/16 comparison (Figure 4D and E). Further, no consistent effect of titration (undiluted → 1/16) was observed for the <10% of BV–BJ combinations whose ΔC_t values fell outside of these ranges suggesting that these shifts were not due to reproducible differences in BV–BJ primer pair efficiences.

Normal T-cell populations exhibit variable levels of expression of both BV and BJ genes (23–26), and it

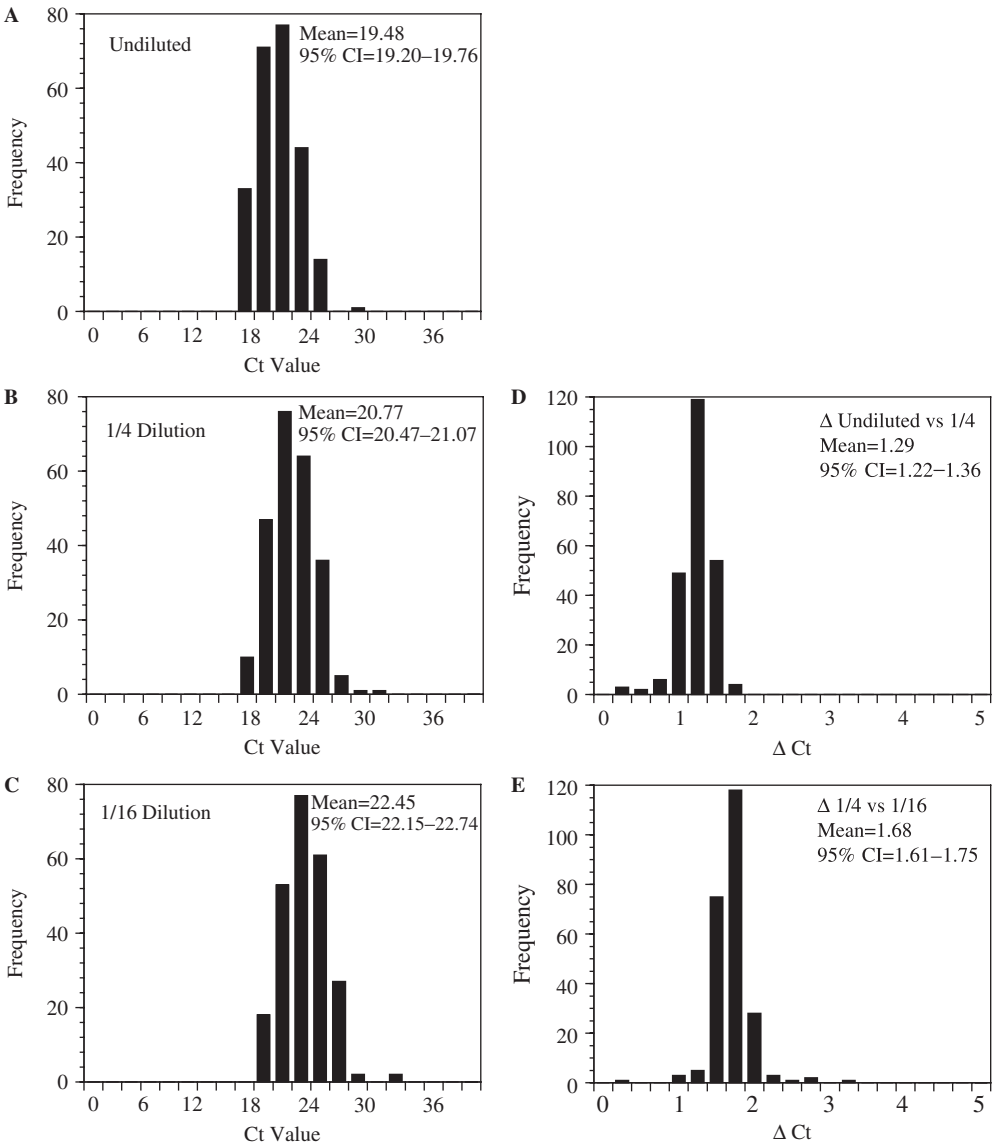

Figure 4. Effects of titration of products of pooled RT–PCRs on BV–BJ-specific amplification in real-time PCRs. β transcripts in total RNA from B6 splenocytes were amplified in pooled RT–PCRs and specific amplicons were enriched with magnetic beads. Enriched products were amplified in BV–BJ-specific real-time reactions after either no dilution (**A**) or dilutions of 1/4 (**B**) and 1/16 (**C**). Comparisons of Ct values from matched BV–BJ-specific amplifications were performed to yield distributions of ΔC_t values and estimations of mean ΔCt values (**D** and **E**).

could be expected that reducing the amount of starting RNA template for the BV–BJ matrix results in the loss of detection of transcripts that carry BV–BJ combinations that are low in abundance. The data presented above suggest that the speed of amplification in the real-time PCR phase of the BV–BJ matrix method is directly related to the amount of bead-enriched template. However, the Ct values in the BV–BJ matrix are the product of amplification in both the real-time PCRs as well as the pooled RT–PCRs. Predictably, the RT–PCRs are more complex reactions given the heterogeneous template and pooled BV primers that potentially could result in non-specific amplification and competition between BV primers for amplification with the biotinylated BC primer. Accordingly, these amplifications may be more sensitive to variations in amounts of template RNA.

We investigated the effects of RNA titration on amplification with BV–BJ primer pairs. Total RNA was extracted from B6 splenocytes and amplified in pooled RT–PCRs after either no dilution or 1/4 and 1/16 dilutions. Bead-enriched templates were then amplified in real-time PCRs to evaluate the effects of RNA template dilution on mean Ct values and ΔC_t values for individual BV–BJ primer pairs. Reductions in amounts of RNA template resulted in increases in mean Ct values (Figure 5A–C) with increased tailing toward higher Ct values with extended (1/16) dilution. Further, the breadths of the major peaks of ΔC_t values were increased following dilution (Figure 5D and E) over those observed with 1/4 and 1/16 dilutions of bead-enriched templates for real-time PCRs (Figure 4D and E). The increases in ΔC_t variability are not unexpected given that template dilutions were

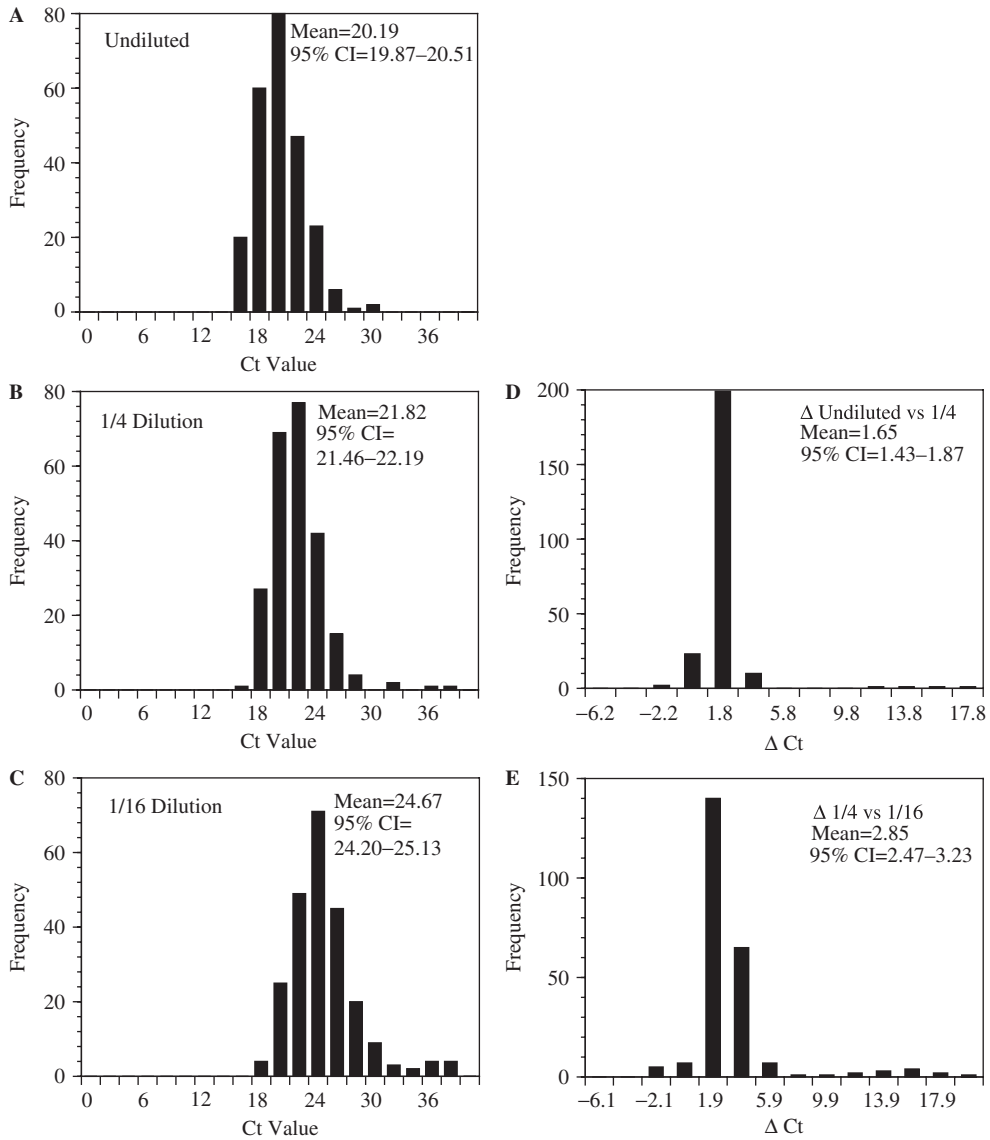

Figure 5. Effects of titration of RNA template on BV–BJ-specific amplification of β transcripts. Total RNA template from B6 splenocytes was amplified in pooled RT–PCRs after no dilution or dilutions of 1/4 and 1/16. Specific amplicons were enriched with magnetic beads and amplified with BV–BJ primer pairs in real-time PCRs. Distributions of Ct values are presented in (**A**) (undiluted), (**B**) (1/4 dilution), and (**C**) (1/16 dilution). Comparisons of Ct values from matched BV–BJ-specific amplifications were performed to yield distributions of ΔCt values and estimations of mean ΔCt values (**D** and **E**).

made prior to the pooled RT–PCRs that utilize total RNA template and multiple, pooled BV primers. This increased variability extended further to a minority (<10%) of BV–BJ combinations that exhibited ΔC_t values (1/4 versus 1/16) that exceeded those expected for a 4-fold dilution. A close examination of the Ct values for these BV–BJ combinations revealed that there was no clear correlation between the Ct values with 1/4 diluted template and their ΔC_t values (1/4 versus 1/16). We investigated the effects of RNA template dilution on Shannon entropy estimates of diversity and calculated scaled entropy values of 0.86, 0.85 and 0.81 for the undiluted, 1/4 diluted and 1/16 diluted RNA templates, respectively. The estimated loss in diversity with increasing template dilution (1/16) appeared to be due to a small number of BV–BJ primer pairs that yielded no amplification (Ct > 40 cycles).

Considering the results of titrations of both bead-enriched template and starting RNA template, it is apparent that amplifications with the vast majority of BV–BJ primer pairs respond concordantly to template titrations. However, data in Figures 4 and 5 show that template can be reduced to an amount where ΔC_ts from a minority of BV–BJ-specific amplifications exceed the values predicted by the template dilution resulting in a loss of representation. Since there is a wide range of representation of transcripts with different BV–BJ combinations, it is important to select amounts of starting RNA for RT–PCRs and bead-enriched templates for real-time PCRs that (i) exceed the amounts required for detection of highly

represented transcripts and (ii) are sufficient for detection of poorly represented transcripts to maximize the observable diversity of BV–BJ combinations.

Detection of variable diversity

The analyses of multiple inbred mice with the BV–BJ matrix have shown that BV–BJ combinations exhibit only minor variations in representation in normal C57 background mice (data not shown). This relative homogeneity may be based in the housing of these genetically identical mice under specific pathogen-free conditions that do not exert significant selective pressures on T-cell populations. The ability of the BV–BJ matrix to detect repertoires with reduced or skewed diversity was investigated through the use of genetically immunocompromized mice and populations of lymphocytes that were purposefully mixed with monoclonal T-cells.

Immunocompromized mice included (i) NOD-scid mice that lack B and T cells and (ii) nude mice that are athymic but capable of low levels of extra-thymic T cell development leading to accumulations of detectable T-cell populations with increasing age (27). Spleens were harvested from nude mice at 16 weeks of age based on previous observations that populations of $CD4^+$ and $CD8^+$ T cells have accumulated by that age (27). B cells were depleted from nude spleen cells by panning over dishes coated with goat anti-mouse Ig. The eluted cells were 50% T cells based on flow cytometric analysis using fluorochrome-labeled antibodies specific for CD3, CD8 and CD4 (data not shown). Total RNA was extracted from these populations and analysed by the BV–BJ matrix (Figure 6B for one representative mouse). The results of the BV–BJ analysis of nude T cells differed from those of normal B10 T cells (Figure 6A) in two principal respects: (i) the median Ct value (23.9 cycles) was 5.4 cycles slower than the median Ct value for normal B10 T cells and (ii) no amplification was observed for 20% of the BV–BJ combinations. The apparent reduction in diversity of the nude TCR repertoire was supported by Shannon entropy analysis that yielded scaled entropy values of 0.88 and 0.73 for normal and nude T cells, respectively. Reduced diversity in the nude BV–BJ matrix was also indicated by the identification of amplicons from the real-time PCRs that had dissociation curves with reduced breadth suggesting reduced complexity. Six amplicons of this type were selected for direct sequencing and four amplicons yielded single-copy sequences for clear translations of the CDR3s (included in Figure 6B). Greater reduction in BV–BJ diversity was observed through analysis of splenocytes from an NOD-scid mouse. NOD-scid mice lack B and T cells due to a mutation in the Prkdc gene (28) so they provide a physiological negative control for the specificities of the BV and BJ primers. Total RNA extracted from whole splenocyte populations were amplified with the BV–BJ matrix method (Figure 6C for one sample). Products were obtained for only six BV–BJ combinations with Ct values ranging from 26.4 to 39.2 cycles. At least one of these products derived from a single transcript as evidenced by the ability to obtain single copy sequence (included in Figure 6C). These six BV–BJ primer pairs did not yield products with the second RNA template (data not shown). These results indicated that the amplifications in the BV–BJ matrix method required RNA extracted from T lymphocytes.

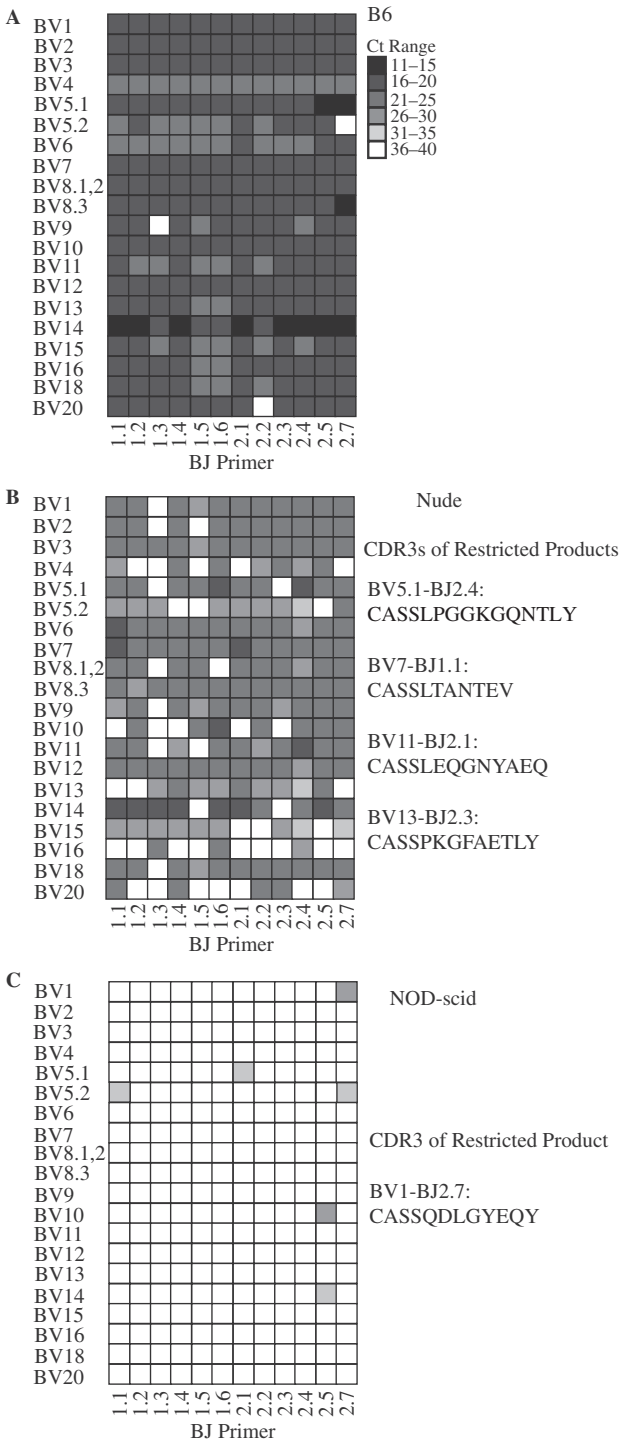

Figure 6. Representations of 240 BV–BJ combinations in RNA extracted from normal and immunodeficient mouse spleen cells. Total RNA was extracted from normal B10 splenocytes (**A**), B cell-depleted nude mouse splenocytes (**B**), and NOD-scid spleen cells (**C**), and amplified by the BV–BJ matrix method. Amplicons with relatively narrow dissociation curves were selected for direct sequencing and the translations of single copy sequences are presented.

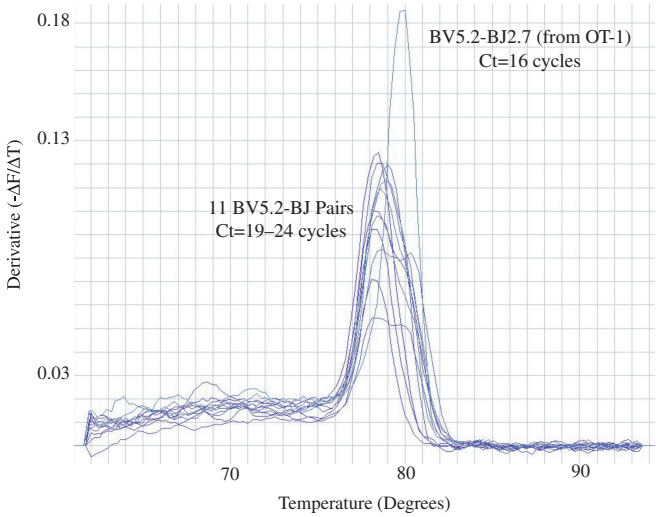

Figure 7. Detection of an experimentally overrepresented transcript by the BV–BJ matrix method. Normal B6 and transgenic OT-1 spleen cells were mixed in a 100:1 ratio prior to the extraction of total RNA. Total RNA template was amplified by the BV–BJ matrix method and the dissociation curves of products amplified by pairings of the BV5.2 primer with the 12 BJ primers are presented. The BV5.2–BJ2.7 amplicons were directly sequenced and the translated sequence matched the CDR3 of the OT-1 β chain.

The identification of single copy sequences in amplicons derived from nude mouse T cells suggests that the BV–BJ matrix method is capable of amplifying and identifying overrepresented transcripts for direct sequencing. An additional test involved the mixing of normal T-cell populations with limited numbers of monoclonal T cells prior to total RNA extraction. Normal B6 spleen cells were mixed in a 100:1 ratio with splenocytes from an OT-1 transgenic mouse whose T cells expressed a BV5.2–BJ2.7 rearrangement (29). Total RNA that was extracted from the mixed cells was amplified in pooled RT–PCRs and re-amplified by real-time PCRs. The dissociation curves for wells combining the BV5.2 primer with the 12 BJ primers are presented in Figure 7. The BV5.2–BJ2.7 primer pair yielded accelerated amplification (Ct = 16 cycles) when compared with Ct values from the other 11 BV5.2–BJ primer pairs (19–24 cycles). Further, the dissociation peak from the BV5.2–BJ2.7 primer pair had increased magnitude and reduced width. This product was directly sequenced and yielded single-copy sequence which translated into the reported OT-1 CDR3 sequence (CASSRANYEQY). These results and those presented above for amplification of RNA from nude mice demonstrate that the BV–BJ matrix has the capacity to identify and ultimately sequence overrepresented TCR β transcripts within whole populations of lymphocytes.

Restricted repertoires in rejecting skin allografts

The separate amplifications of 240 individual BV–BJ combinations should increase the capacity for identifying and sequencing amplicons from overrepresented β transcripts expressed by T-cell populations that infiltrate sites of inflammation. The utility of the BV–BJ matrices for identifying such transcripts was investigated using a model of skin allograft rejection. We have reported that successive sets of skin allografts that are incompatible for a single minor histocompatibility antigen (MiHA) are infiltrated by changing populations of T cells (30). These experiments utilized spectratyping to identify β and α transcripts that were overrepresented at the time of allograft rejection. For the present experiments, we harvested fifth set allografts that expressed either the H4 or HY MiHAs and were in the process of being rejected. Total RNA was extracted from the rejecting allografts and amplified in pooled RT–PCRs and subsequent real-time PCRs.

The matrices from allografts harvested from two recipients for each MiHA (Figures 8 and 9) indicate significantly reduced diversity in comparison to matrices from normal T-cell populations. Specific amplification was observed for only 28–40% (H4) and 60–70% (HY) of the BV–BJ combinations. Ct values were increased over those observed with normal T cells indicating reduced amounts of β transcript templates. In addition, the widths of dissociation curves were highly variable in comparison to those same amplifications of templates from normal mice (Figure 10) suggesting that the amplified products were variable in their complexity. Working under the assumption that the most narrow dissociation peaks included single products, sets of BV–BJ products were selected from the matrices from single recipients for sequencing with the respective BV primers. Single copy sequences with productive rearrangements were obtained for 81% of the sequenced BV–BJ products from both H4- and HY-incompatible grafts (Tables 2 and 3). All sequences included the expected BV sequences indicating that the sequenced BV–BJ amplifications were at least BV-specific. BJ identity was confirmed in 92% of the sequences derived from H4-incompatible grafts, and the remaining sequences included shortened BJ segments. Multiple products were observed with 13 and 12% of the products from H4- and HY-incompatible grafts, respectively, and 5% (H4) and 6% (HY) of the products were non-productive rearrangements. Only 1% of the products could not be sequenced due to low amounts of product. The CDR3s that were derived from the H4-incompatible grafts were inspected for net charges and lengths to compare them to CDR3 sequences that we have previously obtained from multiple sets of H4-incompatible grafts (30). The mean net charges (−0.8) and lengths (8.4 amino acids) were comparable to the CDR3s previously obtained from fifth set grafts.

DISCUSSION

T-cell populations must sustain sufficient diversity to both maintain memory responses as well as mount effective responses by naïve T cells, and the diversity of T-cell populations is determined by the diversity of expressed TCRs. An approach for rigorously evaluating TCR diversity would expectedly offer new opportunities to analyse T-cell repertoires in individuals with compromized or reconstituted immune systems. Such an approach should also find increased utility in the analysis of T-cell populations that infiltrate sites of autoimmunity, rejection of

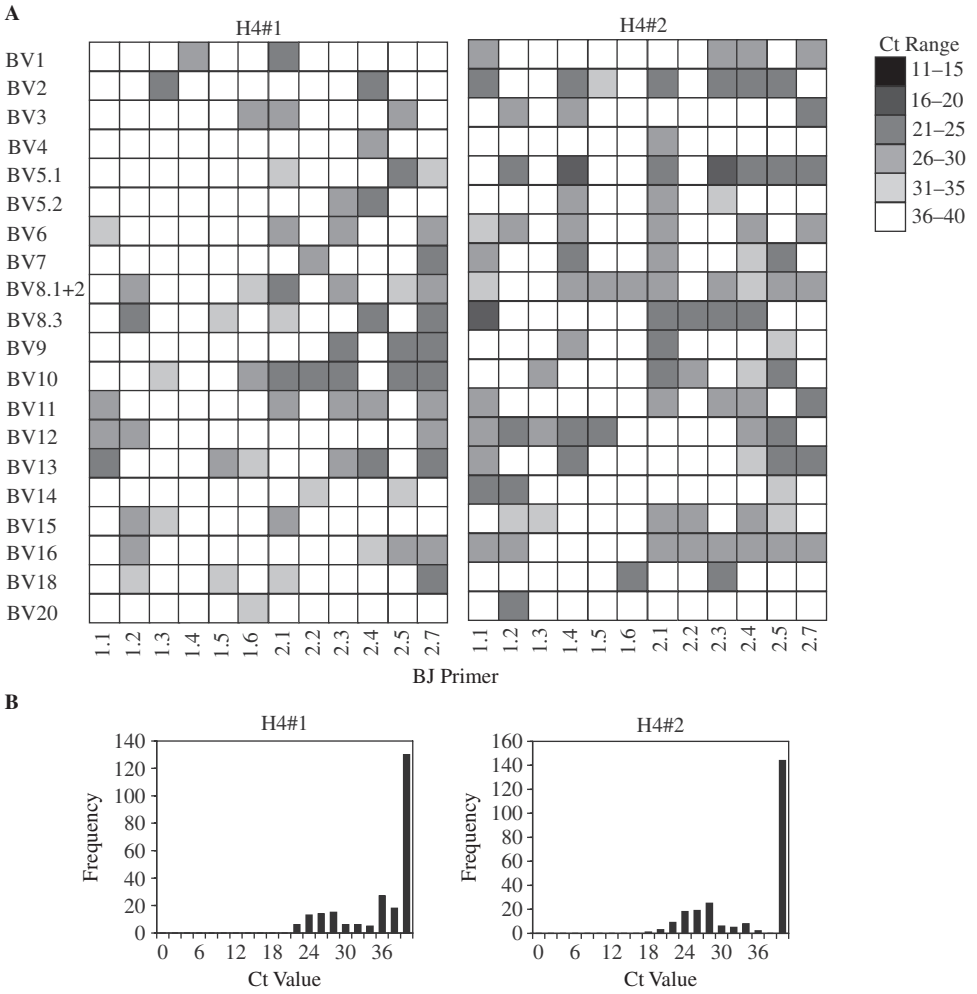

Figure 8. Representations of 240 BV–BJ combinations in RNA extracted from H4-incompatible skin grafts at the times of rejection by two recipients. (**A**) Distributions of Ct values for individual BV–BJ-specific amplifications and (**B**) frequency distributions of Ct values.

transplants and elimination of tumors, in order to provide information on the diversity of infiltrating T cells. Spectratyping has played an essential role in these analyses but appears to be somewhat limited in broad, clinical applications due to a number of limitations. The method is relatively time-consuming and generates data that are difficult to statistically evaluate since the data are spectra of CDR3 lengths that are generated by gel electrophoresis and are highly variable in amplitude and length distribution. The analysis of diversity has generally been performed by visual inspection of the data, and a statistical method has been reported for identifying significant skewing in spectratypes but not comparing diversities of different RNA templates (31). The identification of overrepresented β transcripts is limited by the BV gene-specific amplifications; with this level of resolution, the identification of a single, overrepresented transcript requires that expression of a single BV gene be limited to a single, predominant T-cell clonotype. The efficiency of identification of overrepresented transcripts by spectratyping has been increased by re-amplification with BJ primers (15), but this approach is not amenable to routine monitoring of repertoire diversity due to cost and labor intensity. Alternative methods have been reported for evaluating repertoire diversity through quantitation of (i) re-annealing of amplicons from β transcripts (7,8) and (ii) hybridization of β transcript cRNAs to arrays of oligonucleotides that are unrelated to β transcripts (9). It is certainly not clear that the former methods can be extended to the analysis of total repertoires rather than limited subsets of β transcripts, i.e. specific BV–BJ combinations, and the statistical methods for analyzing the data produced by these assays have not been clearly described. Even if these limitations are overcome, these methods are still restricted to analysis of diversity of T-cell populations without any possibility of identifying and sequencing overrepresented transcripts.

The BV–BJ matrix method was designed to efficiently analyse the diversities of β transcript repertoires and maximize identification and sequencing of overrepresented β transcripts. The use of real-time PCR instrumentation for analysis of TCR repertoires offers a number of improvements in sensitivity, sample handling, data acquisition and data analysis. First, the simultaneous monitoring of

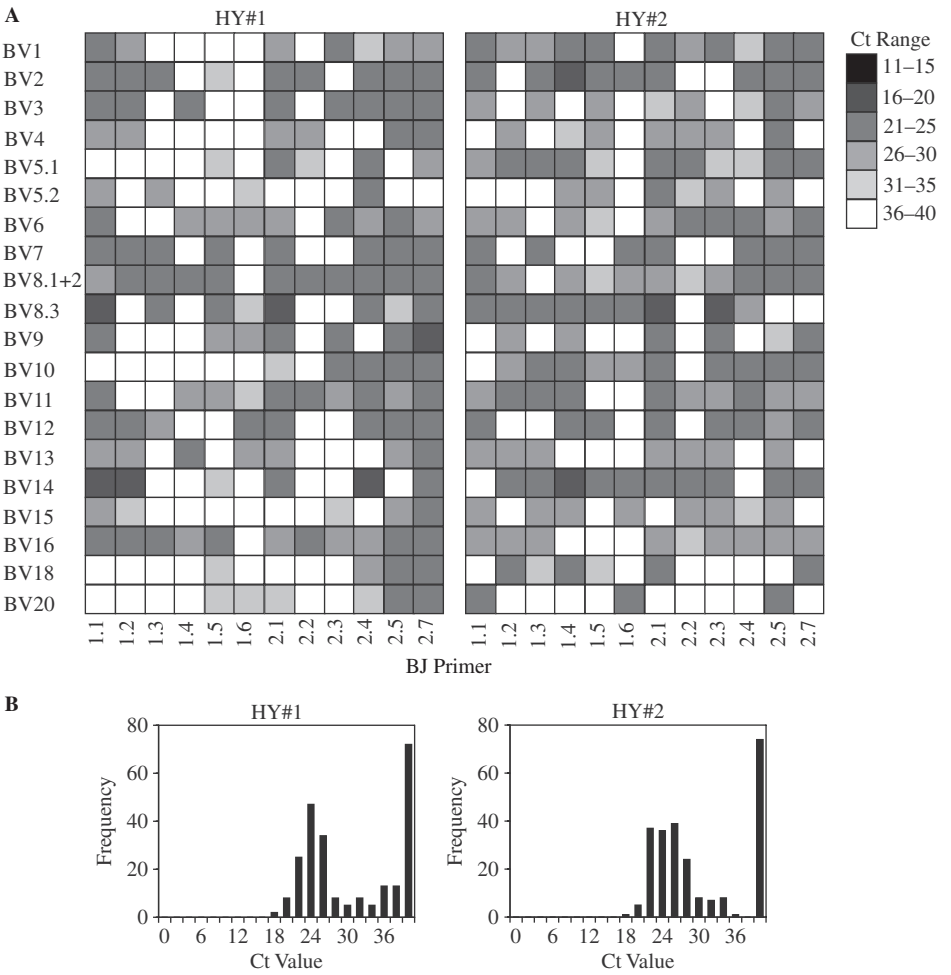

Figure 9. Representations of 240 BV–BJ combinations in RNA extracted from HY-incompatible skin grafts at the times of rejection by two female recipients. (**A**) Distributions of Ct values for individual BV–BJ-specific amplifications and (**B**) frequency distributions of Ct values.

amplification in all reactions through incorporation of SYBR Green provides estimates of the tempo of amplification throughout entire reactions with estimations of Ct values. Second, automated melting at the completion of the reactions provides dissociation curves for confirming specific amplification. These automated analyses eliminate the additional sample handling and electrophoretic separation required in spectratyping for identification, separation and quantitation of products. Third, the simultaneous analysis of amplification with a single matrix of BV–BJ primer pairs simplifies data organization and statistical analysis. The dissection of β transcript repertoires with a matrix of defined BV–BJ combinations enabled us to estimate relative β transcript diversities by Shannon entropy that has been used previously to estimate the variability of individual amino acid positions in the variable regions of immunoglobulin heavy chains and TCR β chains (22,32). The relatively large number of BV–BJ primer pairs increases the sensitivity of Shannon entropy (21), and continuous Ct values, rather than simple 'presence' or 'absence' of amplification, increase the amount of information in these diversity estimates. Fourth, the increased resolution associated with 240 BV–BJ combinations improves the efficiency of identifying and sequencing overrepresented transcripts due to the increased number of individual PCRs that increases the probability of isolating products derived from single, prominent β transcripts. Regarding the specificity of amplification with the BV–BJ matrix, products from 131/240 BV–BJ primer pairs have now been sequenced with 100% fidelity for BV and BJ genes (Figures 8 and 9; and data not shown). All 21 BV genes are represented in this set of sequenced products, thereby confirming the specificity of all nested BV primer pairs.

In addition to these methodological advantages, the use of BV–BJ primer pairs in real-time PCRs constitutes a fundamentally different approach to analyzing the diversity of β transcripts expressed by T-cell populations. TCRs recognize peptides bound by MHC molecules with specificity being directed toward both MHC molecules and bound peptides. V regions of TCR α and β subunits bind principally to MHC molecules through CDR1 and CDR2 regions with limited, if any, direct contact with bound peptides, and J regions have limited contacts with MHC + peptide (33). CDR3s in the α and β subunits provide the major contacts with MHC-bound peptides so CDR3 motifs and lengths are important in determining specificity for these peptides (6,33). In fact, restriction in

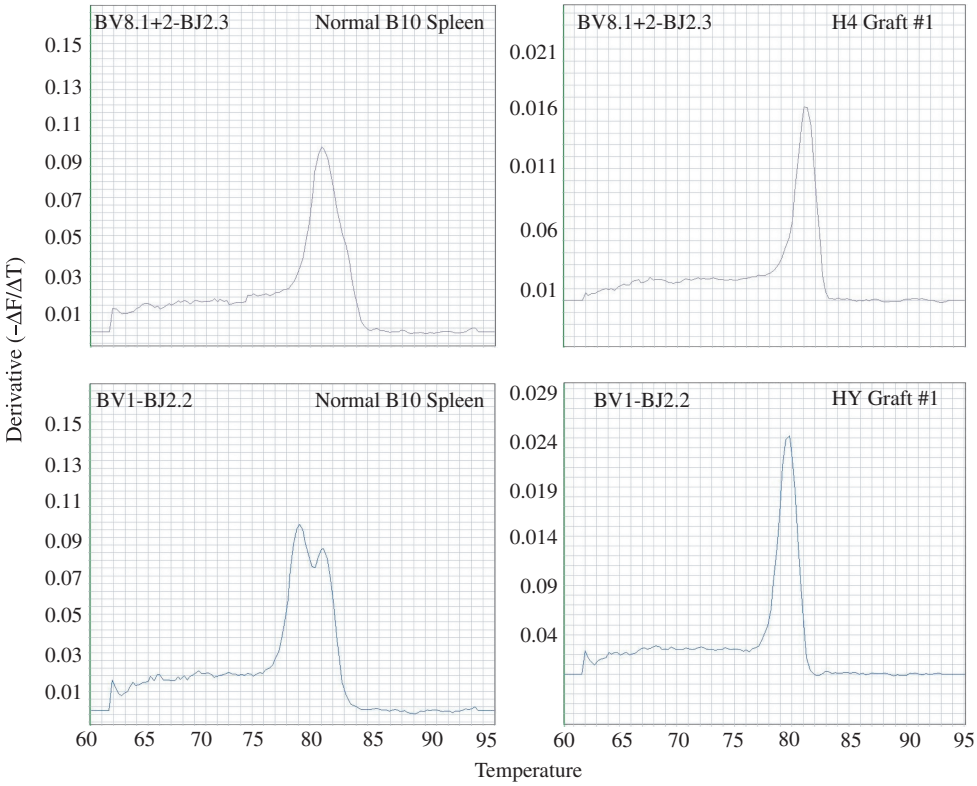

Figure 10. Dissociation curves from products of BV–BJ-specific amplications of total RNA from normal splenocytes and rejecting allografts.

CDR3 length has been reported to be the first CDR3 characteristic to be selected in murine T cell responses (4). Spectratyping principally focuses on evaluating repertoire diversity with distributions of CDR3 lengths in transcripts carrying individual BV genes. The presence of restricted or skewed distributions of CDR3 lengths are considered to be indicative of restriction of TCR repertoires presumably through the presence of T clonotypes that have expanded in responses to specific antigens. Studies in mice and humans have shown that the majority of predominant peaks with single CDR3 lengths are comprised of products amplified from multiple β transcripts (34,35), suggesting that evaluation of repertoire diversity by CDR3 length distribution alone could lead to underestimation of diversity. However, the more limited involvement of BV and BJ regions in direct contacts with MHC-bound peptides should limit the selection of individual BV–BJ combinations in expansions of T-cell clonotypes in antigen-specific responses. T-cell subpopulations that respond to single peptides appear to express diverse BV and BJ combinations relative to the more restricted CDR3 lengths and motifs, although there are a number of peptides in experimental models that appear to stimulate T cells with restricted BV usage (3,5). Therefore, dissection of T-cell repertoires by estimating the distribution of individual BV–BJ combinations should provide estimates of repertoire diversity with reduced biases from previous clonotypic expansions. Amplification of β transcripts with an array of individual BV–BJ primer pairs still facilitates identification of oligoclonal expansions of T-cell clonotypes within total T-cell populations (Figures 6 and 7).

The BV–BJ matrix method is not without its own technical difficulties and shortcomings. First, it does not reveal skewing of CDR3 length distributions that may indicate previous *in vivo* priming of T-cell subpopulations. However, the products amplified in BV–BJ matrices could certainly be electrophoretically separated to yield spectra of CDR3 lengths within amplicon populations carrying single BV–BJ combinations. Second, the sensitivity of real-time PCR analysis of TCR repertoires to amounts of starting template and amplification conditions requires careful estimation of percentages of T cells and control of amplification conditions. Routine use of the described method to compare levels of diversity in total T-cell populations should involve enrichment of T cells or $CD4^+$ and $CD8^+$ subpopulations to ensure that percentages of T cells within the populations used for RNA extractions are consistent. Successful control over amplification conditions requires normalization, but the amplification of only ~0.4% of available β transcripts by individual pairs of BV–BJ primers complicates such normalization that is routinely achieved by amplification with primers specific for unrelated genes that are transcribed at levels comparable to the genes whose transcripts are being analysed. Experiments are in progress to develop rigorous normalization methods for RT–PCRs and BV–BJ matrices to monitor variations in amplification conditions by using total RNA templates that are diluted to yield Ct values that are comparable to those obtained with BV–BJ

Table 2. Amino acid sequences of β CDR3s that are overrepresented in H4-incompatible skin grafts at the time of rejection by a single recipient (H41)

BV–BJ pair	BV–CDR3–BJ sequence		
BV1–BJ2.3	CASS	LDWGG	AETLYFGSGTRLTVL
BV1–BJ2.4	CASS	SQDWG	QNTLYFGAGTRLSVL
BV1–BJ2.7	CASS	SDRV	QYFGPGTRLTVL
BV2–BJ1.1	CSA	DRPGAS	TEVFFGKGTRLTVV
BV2–BJ1.4	CSA	GTT	NERLFFGHGTKLSVL
BV2–BJ2.1	CS	V	NYAEQFFGPGTRLTVL
BV2–BJ2.5	CSA	DCS	QDTQYFGPGTRLLVL
BV3–BJ1.2	CASS	RT	NSDYTFGSGTRLLVI
BV3–BJ1.4	CAG	TGGP	NERLFFGHGTKLSVL
BV3–BJ2.1	CASS	LSGR	AEQFFGPGTRLTVL
BV3–BJ2.7	CASS	LGDD	EQYFGPGTRLTVL
BV5.1–BJ1.2	CASS	QG	NSDYTFGSGTRLLVI
BV5.1–BJ1.4	CASS	LERG	SNERLFFGHGTKLSVL
BV5.1–BJ2.1	CASS	PGLG	YAEQFFGPGTRLTVL
BV5.1–BJ2.4	CASS	LALGG	SQNTLYFGAGTRLSVL
BV5.1–BJ2.7	CASS	LAGGG	YEQQFGPGTRLTVL
BV6–BJ1.1	CASS	FGQGA	EVFFGKGTRLTVV
BV6–BJ1.2	CASS	IRD	SDYTFGSGTRLLVI
BV6–BJ2.1	CASS	IRD	NYAEQFFGPGTRLTVL
BV7–BJ1.1	CASP	QVA	NTEVFFGKGTRLTVV
BV7–BJ2.5	CASS	PGQG	DTQYFGPGTRLLVL
BV8.1–BJ2.1	CASS	DQGD	YAEQFFGPGTRLTVL
BV8.1–BJ2.5	CASS	GTG	QDTQYFGPGTRLLVL
BV8.2–BJ1.5	CASG	VQGG	NQAPLFGEGTRLSVL
BV8.2–BJ2.3	CASG	DLGG	SAETLYFGSGTRLTVL
BV8.3–BJ1.1	CASS	DGTV	EVFFGKGTRLTVV
BV8.3–BJ1.2	CASR	GPA	NSDYTFGSGTRLLVI
BV8.3–BJ2.2	CASS	E	NTGQLYFGEGSKLTVL
BV8.3–BJ2.4	CASS	DWGF	QNTLYFGAGTRLSVL
BV9–BJ2.5	CASS	RDTGAR	DTQYFGPGTRLLVL
BV10–BJ1.3	CASS	GRS	SGNTLYFGEGSRLIVV
BV10–BJ2.2	CASS	LDWR	NTGQLYFGEGSKLTVL
BV11–BJ1.1	CASS	LGNA	NTEVFFGKGTRLTVV
BV11–BJ1.3	CASS	LGT	SGNTLYFGEGSRLIVV
BV11–BJ2.3	CASS	PGTG	AETLYFGSGTRLTVL
BV11–BJ2.4	CASS	LEPD	SQNTLYFGAGTRLSVL
BV12–BJ1.2	CASS	S	NSDYTFGSGTRLLVI
BV12–BJ1.3	CASS	DRA	GNTLYFGEGSRLIVV
BV12–BJ1.5	CASS	WTG	NQAPLFGEGTRLSVL
BV12–BJ2.4	CASS	LD	SQNTLYFGAGTRLSVL
BV12–BJ2.5	CASS	LYE	DTQYFGPGTRLLVL
BV13–BJ1.1	CASS	PRDR	NTEVFFGKGTRLTVV
BV13–BJ1.4	CASS	LQGD	NERLFFGHGTKLSVL
BV13–BJ2.5	CASS	LWGD	QDTQYFGPGTRLLVL
BV14–BJ1.1	CAWS	PPGT	NTEVFFGKGTRLTVV
BV14–BJ1.2	CAWS	LPGQGD	SDYTFGSGTRLLVI
BV15–BJ2.1	CGAR	DRQ	NYAEQFFGPGTRLTVL
BV15–BJ2.4	CGAR	GR	QNTLYFGAGTRLSVL
BV16–BJ1.1	CASS	QANK	EVFFGKGTRLTVV
BV18–BJ1.6	CSS	NNRG	YNSPLYFAAGTRLTVT
BV18–BJ2.3	CS	PRDWGA	SAETLYFGSGTRLTVL
BV20–BJ1.2	CSSS	WDRA	SDYTFGSGTRLLVI

Table 3. Amino acid sequences of β CDR3s that are overrepresented in HY-incompatible skin grafts at the time of rejection by a single recipient (HY1)

BV–BJ pair	BV–CDR3–BJ sequence		
BV1–BJ1.5	CASS	QEGGI	QAPLFGEGTRLSVL
BV1–BJ2.4	CASS	QGGIN	QNTLYFGAGTRLSV
BV2–BJ1.3	CSA	TEV	SGNTLYFGEGSRLIVV
BV2–BJ1.4	CS	GNGQG	SNERLFFGHGTKLSVL
BV2–BJ1.5	CSA	QG	NNQAPLFGEGTRLSVL
BV2–BJ2.4	CRA	GRRG	SQNTLYFGAGTRLSVL
BV3–BJ1.1	CASS	LSQ	NTEVFFGKGTRLTVV
BV3–BJ2.2	CASS	RTD	TGQLYFGEGSKLTVL
BV3–BJ2.7	CASS	LNRG	EQYFGPGTRLTVL
BV5.1–BJ2.1	CASS	LNWGD	AEQFFGPGTRLTVL
BV5.1–BJ2.2	CASS	LSGY	TGQLYFGEGSKLTVL
BV5.1–BJ2.5	CASW	G	NQDTQYFGPGTRLLVL
BV5.2–BJ1.5	CASS	PDS	NNQAPLFGEGTRLSVL
BV5.2–BJ2.3	CASS	LGGA	SAETLYFGSGTRLTVL
BV5.2–BJ2.5	CASS	RTV	NQDTQYFGPGTRLLVL
BV6–BJ1.2	CASS	MGQEA	SDYTFGSGTRLLVI
BV6–BJ2.1	CASS	RGS	YAEQFFGPGTRLTVL
BV6–BJ2.2	CASS	LPGG	TGQLYFGEGSKLTVL
BV7–BJ1.1	CASS	FSRS	NTEVFFGKGTRLTVV
BV7–BJ2.7	CASS	WGWR	YEQYFGPGTRLTVL
BV8.1–BJ2.2	CASS	DRSD	TGQLYFGEGSKLTVL
BV8.2–BJ1.4	CASA	RDT	NERLFFGHGTKLSVL
BV8.2–BJ2.3	CASG	GTT	SAETLYFGSGTRLTVL
BV8.3–BJ1.2	CASS	DAH	SDYTFGSGTRLLVI
BV8.3–BJ1.5	CASS	RES	NQAPLFGEGTRLSVL
BV8.3–BJ2.1	CASS	DEDWA	YAEQFFGPGTRLTVL
BV9–BJ1.4	CASS	TGGAA	NERLFFGHGTKLSVL
BV9–BJ2.3	CASR	RRGR	AETLYFGSGTRLTVL
BV10–BJ1.5	CASS	DRY	NNQAPLFGEGTRLSVL
BV10–BJ1.6	CASR	RTF	SYNSPLYFAAGTRLTVT
BV10–BJ2.7	CASS	YP	YEQYFGPGTRLTVL
BV11–BJ1.3	CASS	NRGL	GNTLYFGEGSRLIVV
BV11–BJ1.4	CASS	LVERSK	ERLFFGHGTKLSVL
BV11–BJ2.3	CASR	AGGS	SAETLYFGSGTRLTVL
BV12–BJ1.5	CASS	LGR	NQAPLFGEGTRLSVL
BV12–BJ2.1	CASS	LSGGD	AEQFFGPGTRLTVL
BV12–BJ2.4	CASS	TQ	SQNTLYFGAGTRLSVL
BV13–BJ1.2	CASS	LTG	NSDYTFGSGTRLLVI
BV13–BJ2.1	CASS	FWGD	YAEQFFGPGTRLTVL
BV13–BJ2.5	CASS	FTG	QDTQYFGPGTRLLVL
BV14–BJ1.5	CAWR	QRV	NNQAPLFGEGTRLSVL
BV14–BJ1.6	CAWS	RG	SYNSPLYFAAGTRLTVT
BV14–BJ2.1	CAWS	RRV	NYAEQFFGPGTRLTVL
BV14–BJ2.5	CAWS	LRLGA	QDTQYFGPGTRLLVL
BV15–BJ1.3	CGA	RDRVF	GNTLYFGEGSRLIVV
BV15–BJ1.4	CGAG	QGT	NERLFFGHGTKLSVL
BV15–BJ1.6	CGA	RDG	YNSPLYFAAGTRLTVT
BV18–BJ1.2	CSSR	DSA	NSKYTFGSGTRLLVI
BV18–BJ1.4	CSSR	GTGRG	ERLFFGHGTKLSVL
BV18–BJ2.1	CSSR	ANS	YAEQFFGPGTRLTVL
BV18–BJ2.7	CSSR	GGC	YEQYFGPGTRLTV
BV20–BJ1.1	CSSS	LQG	TEVFFGKGTRLTVV
BV20–BJ1.6	CSSS	QLAD	NSPLYFAAGTRLTVT
BV20–BJ2.5	CSSS	QRTGGR	DTQYFGPGTRLLV

primer pairs. Further, routine analysis should include the use of negative control cells, e.g. fibroblasts, to confirm specificity of amplification and detect any cross-contamination.

The data presented in Figure 5 show that extended dilutions of total RNA templates may result in speeds of amplification that are slower than expected for the range of dilutions, and the numbers of BV–BJ combinations that exhibit such decreased amplification increase with extended dilutions. These dilution effects would also be expected with spectratyping but may be difficult to identify given that electrophoretic separations of products with complex and variable length distributions complicate analysis. It follows that direct comparisons of TCR repertoire diversities in whole T-cell populations versus tissue-infiltrating T cells should be avoided unless the latter lymphocytes are enriched before total RNA extraction. Such comparisons have been previously reported to show T-cell oligoclonality in biopsies of human inflammatory sites

including melanomas and head and neck cancers (12,36). Although those analyses most certainly identified overrepresented transcripts, TCR diversity may have been under-estimated given that enrichments of infiltrating T cells were not performed.

The BV–BJ matrices are presently being developed for analysis of repertoires of human T-cell populations. Humans express 47 BV genes and 13 BJ genes (37), and these numbers require increased attention to the design of BV-specific nested primers since the majority of BV genes are closely related members of subfamilies (37). The resulting matrices of 611 individual BV–BJ combinations will provide even greater resolution than the mouse matrices and increase the efficiency of identifying and sequencing β transcripts from sites of T-cell infiltration. We believe that BV–BJ matrices have the potential to accelerate the analyses of T-cell repertoires in humans and animal models through their technical simplicity, increased levels of resolution and uncomplicated statistical analysis.

ACKNOWLEDGEMENT

The authors gratefully acknowledge the assistance of Ms DeAnn Frederixon for graphic presentations.

FUNDING

Funding for open access charge: Mayo Clinic Funds.

Conflict of interest statement. None declared.

REFERENCES

1. Chien,Y.H., Gascoigne,R.J., Kavaler,J., Lee,N.E. and Davis,M.M. (1984) Somatic recombination in a murine T-cell receptor gene. *Nature*, **309**, 322–326.
2. McHeyzer-Williams,M.G. and Davis,M.M. (1995) Antigen-specific development of primary and memory T cells in vivo. *Science*, **268**, 106–111.
3. Kedzierska,K., La Gruta,N.L., Davenport,M.P., Turner,S.J. and Doherty,P.C. (2005) Contribution of T cell receptor affinity to overall avidity for virus-specific $CD8^+$ T cell responses. *Proc. Natl Acad. Sci. USA*, **102**, 11432–11437.
4. McHeyzer-Williams,L.J., Panus,J.F., Mikszta,J.A. and McHeyzer-Williams,M.G. (1999) Evolution of antigen-specific T cell receptors in vivo: preimmune and antigen-driven selection of preferred complementarity-determining region 3 (CDR3) motifs. *J. Exp. Med.*, **189**, 1823–1837.
5. Zhong,W. and Reinherz,E.L. (2004) In vivo selection of a TCR Vβ repertoire directed against an immunodominant influenza virus CTL epitope. *Intl Immunol.*, **16**, 1549–1559.
6. Garcia,K.C., Degano,M., Pease,L.R., Huang,M., Peterson,P.A., Teyton,L. and Wilson,I.A. (1998) Structural basis of plasticity in T cell receptor recognition of a self peptide-MHC antigen. *Science*, **279**, 1166–1172.
7. Wagner,U.G., Koetz,K., Weyand,C.M. and Goronzy,J.J. (1998) Perturbation of the T cell repertoire in rheumatoid arthritis. *Proc. Natl Acad. Sci. USA*, **95**, 14447–14452.
8. Baum,P.D. and McCune,J.M. (2006) Direct measurement of T-cell receptor repertoire diversity with AmpliCot. *Nat. Methods*, **3**, 895–901.
9. Ogle,B.M., Cascalho,M., Joao,C., Taylor,W., West,L.J. and Platt,J.L. (2003) Direct measurement of lymphocyte receptor diversity. *Nucleic Acids Res.*, **31**, e139.
10. Pannetier,C., Cochet,M., Darche,S., Casrouge,A., Zoller,M. and Kourilsky,P. (1993) The sizes of the CDR3 hypervariable regions of the murine T-cell receptor β chains vary as a function of the recombined germ-line segments. *Proc. Natl Acad. Sci. USA*, **90**, 4319–4323.
11. DePalma,R. and Gorsky,J. (1995) Restricted and conserved T-cell repertoires involved in allorecognition of class II major histocompatibility complex. *Proc. Natl Acad. Sci. USA*, **92**, 8836–8840.
12. Caignard,A., Dietrich,P., Morand,V., Lim,A., Pannetier,C., Leridant,A.M., Hercend,T., Even,J., Kourilsky,P. and Triebel,F. (1994) Evidence for T-cell clonal expansion in a patient with squamous cell carcinoma of the head and neck. *Cancer Res.*, **54**, 1292–1297.
13. Musette,P., Bequet,D., Delarbre,C., Gachelin,G., Kourilsky,P. and Dormont,D. (1996) Expansion of a recurrent Vβ5.3+ T-cell population in newly diagnosed and untreated HLA-DR2 multiple sclerosis patients. *Proc. Natl Acad. Sci. USA*, **93**, 12461–12466.
14. Guillet,M., Brouard,S., Gagne,K., Sebille,F., Cuturi,M.C., Delsuc,M.A. and Soulillou,J.P. (2002) Different qualitative and quantitative regulation of Vβ TCR transcripts during early acute allograft rejection and tolerance induction. *J. Immunol.*, **168**, 5088–5095.
15. Pannetier,C., Levraud,J.P., Lim,A., Even,J. and Kourilsky,P. (1997) The immunoscope approach for the analysis of T cell repertoires. In Oksenberg,J.R. (ed), *The Antigen T cell Receptor: Selected Protocols and Applications,* R.G. Landes Company, Georgetown, TX, pp. 287–325.
16. Yassai,M., Naumova,E. and Gorski,J. (1997) Generation of TCR spectratypes by multiplex PCR for T cell repertoire analysis. In Oksenberg,J. R. (ed), *The Antigen T Cell Receptor: Selected Protocols and Applications,* R.G. Landes Company, Georgetown, TX, pp. 326–372.
17. Sriram,U., Wong,M., Caillier,S.J., Hecht,F.M., Elkins,M.K., Levy,J.A., Oksenberg,J.R. and Baranzini,S.E. (2007) Quantitative longitudinal analysis of T cell receptor repertoire expression in HIV-infected patients on antiretroviral and interleukin-2 therapy. *AIDS Res. Human Retroviruses*, **23**, 741–747.
18. Manuel,E.R., Charini,W.A., Sen,P., Peyerl,F.W., Kuroda,M.J., Schmitz,J.E., Autissier,P., Sheeter,D.A., Torbett,B.E. and Letvin,N.L. (2006) Contribution of T-cell receptor repertoire breadth to the dominance of epitope-specific $CD8^+$ T-lymphocyte responses. *J. Virol.*, **80**, 12032–12040.
19. Wysocki,L.J. and Sato,V.L. (1978) "Panning" for lymphocytes: a method for cell selection. *Proc. Natl Acad. Sci. USA*, **75**, 2844–2848.
20. Bailey,D.W. and Usama,B. (1960) A rapid method of grafting skin on tails of mice. *Transplant. Bull.*, **7**, 424–428.
21. Shannon,C.E. (1948) The mathematical theory of communication. *Bell Syst Tech J*, **27**, 379–423, 623–656.
22. Litwin,S. and Jores,R. (1992) Shannon information as a measure of amino acid diversity. In Perelson,A.S. and Weisbuch,G. (eds), *Theoretical and Experimental Insights into Immunology,* Springer, Berlin.
23. Vacchio,M.S. and Hodes,R.J. (1989) Selective decreases in T cell receptor Vβ expression - decreased expression of specific Vβ families is associated with expression of multiple MHC and non-MHC gene products. *J. Exp. Med.*, **170**, 1335–1346.
24. Pullen,A.M., Potts,W., Wakeland,E.K., Kappler,J. and Marrack,P. (1990) Surprisingly uneven distribution of the T cell receptor Vβ repertoire in wild mice. *J. Exp. Med.*, **171**, 49–62.
25. Candeias,S., Waltzinger,C., Benoist,C. and Mathis,D. (1991) The $V\beta17^+$ T cell repertoire: Skewed Jβ usage after thymic selection; dissimilar CDR3s in $CD4^+$ versus $CD8^+$ cells. *J. Exp. Med.*, **174**, 989–1000.
26. Kato,T., Suzuki,S., Sasakawa,H., Masuko,K., Ikeda,Y., Nishioka,K. and Yamamoto,K. (1994) Comparison of the Jβ gene usage among different T cell receptor Vβ families in spleens of CD57BL/6 mice. *Eur. J. Immunol.*, **24**, 2410–2414.
27. Kennedy,J.D., Pierce,C.W. and Lake,J.P. (1992) Extrathymic T cell maturation. Phenotypic analysis of T cell subsets in nude mice as a function of age. *J. Immunol.*, **148**, 1620–1629.
28. Bosma,M., Schuler,W. and Bosma,G. (1988) The scid mouse mutant. *Curr. Top. Microbiol. Immunol.*, **137**, 197–202.
29. Hogquist,K.A., Jameson,S.C., Heath,W.R., Howard,J.L., Bevan,M.J. and Carbone,F.R. (1994) T cell receptor antagonist peptides induce positive selection. *Cell*, **76**, 17–27.

30. Wettstein,P.J., Strausbauch,M. and Borson,N.D. (2007) Repertoires of T cell receptors expressed by graft-infiltrating T cells evolve during long-term recall responses to single minor histocompatibility antigens. *Int. Immunol.*, **19**, 523–534.
31. Killian,M.S., Matud,J., Detels,R., Giorgi,J.V. and Jamieson,B.D. (2002) MaGiK method of T cell receptor repertoire analysis. *Clini. Vacc. Immunol.*, **9**, 858–63.
32. Stewart,J.J., Lee,C., Ibrahim,S., Watts,P., Shlomchik,M., Weigert,M. and Litwin,S. (1997) A Shannon entropy analysis of immunoglobulin and T cell receptor. *Mol. Immunol.*, **34**, 1067–1082.
33. Colf,L.A., Bankovich,A.J., Hanick,N.A., Bowerman,N.A., Jones,L.L., Kranz,D.M. and Garcia,K.C. (2007) How a single T cell receptor recognizes both self and foreign MHC. *Cell*, **129**, 135–146.
34. Naumov,Y.N., Hogan,K.T., Naumova,E.N., Pagel,J.T. and Gorski,J. (1998) A class I MHC-restricted recall response to a viral peptide is highly polyclonal despite stringent CDR3 selection: Implications for establishing memory T cell repertoires in "real-world" conditions. *J. Immunol.*, **160**, 2842–2852.
35. Sourdive,D.J.D., Murali-Krishna,K., Altman,J.D., Zajac,A.J., Whitmire,J.K., Pannetier,C., Kourilsky,P., Evavold,B., Sette,A. and Ahmed,R. (1998) Conserved T cell receptor repertoire in primary and memory CD8 T cell responses to an acute viral infection. *J. Exp. Med.*, **188**, 71–82.
36. Puisieux,I., Even,J., Pannetier,C., Jotereau,F., Favrot,M. and Kourilsky,P. (1994) Oligoclonality of tumor-infiltrating lymphocytes from human melanomas. *J. Immunol.*, **153**, 2807–2818.
37. Giudicelli,V., Chaume,D. and Lefranc,M.P. (2005) IMGT/GENE-DB: a comprehensive database for human and mouse immunoglobulin and T cell receptor genes. *Nucleic Acids Res.*, **33**, D256–D261.